3D Measurements of the Geometry, Internal Flow and Emerging Fuel Jet from the ECN Spray C Injector

Brandon Sforzo*, Aniket Tekawade, Katarzyna E. Matusik,
Alan L. Kastengren, Christopher F. Powell
Argonne National Laboratory, Lemont, IL, USA
*Corresponding author: bsforzo@anl.gov

Abstract
A suite of X-Ray diagnostics has been used to characterize the geometry and internal flow of the Engine Combustion Network "Spray C" diesel injector. X-Ray tomography has been used to determine the geometry of the internal flow passages of this single-hole injector with a spatial resolution better than 2 micrometers. X-ray phase contrast imaging has captured the three-dimensional shape of the cavitation layer that is generated by the sharp inlet and cylindrical shape of this steel nozzle. Finally, time-resolved X-ray tomography has been used to measure the density distribution of the fuel as it first emerges from the nozzle, and its breakup as it moves downstream.

Measurements of the nozzle geometry reveal that the radius of curvature of the inlet corner varies significantly around the azimuthal rotation angle, with a change in radius of as much as 40%. The variation in radius of curvature strongly influences the shape of the cavitation layer that is generated just downstream. The measurements reveal that the cavitation layer inside this nozzle has a highly asymmetric shape, and that the length and thickness of the cavitation sheet are directly tied to the inlet corner radius. At some azimuthal locations, the cavitation layer extends the full length of the nozzle to the outlet, likely causing hydraulic flip and stabilization of the flow separation.

Time-resolved X-ray tomography reveals the impact that the cavitation inside this nozzle has on the fuel distribution. The fuel distribution is highly asymmetric, with a region of very low fuel density that exactly matches the location of greatest cavitation. Together, these measurements form a unique, comprehensive study of cavitation in a cylindrical steel nozzle, from its onset to its manifestation in the external spray.

Keywords
Sprays, Atomization, Fuel Injection, Cavitation, Radiography

Introduction

The measurement of fluid flow inside injection nozzles is critical for the fundamental understanding of fuel systems and the development of combustion engines with high efficiency and low emissions. In particular, cavitation has been found to have a strong impact on the external fuel distribution and fuel and air mixing [1-4]. However, there are significant challenges when trying to measure these flows in nozzles with realistic size, geometry, material, and temperature [5].

A number of studies have gained deep insights into cavitating flows using optically accessible nozzles with a circular cross-sectional geometry. These include measurements on large-scale devices [6,7] as well as real-scale devices with transparent windows [7] or fully-transparent injector tips [8].These measurements preserve the round cross section of the production injector geometry. However, these studies can be hampered by cavitation forming on the front or rear wall of the nozzle, since the multiphase flow in these regions can strongly scatter visible light and obscure the view of the three-dimensional flow structure.

Because this scattering can obscure the cavitation distribution in nozzles with a circular cross section, a number of studies have imaged cavitation in so-called 2D geometries. These nozzles have a rectangular cross section designed to suppress cavitation on the nozzle walls parallel to the imaging plane, while giving a clear view of the cavitation occurring on the walls perpendicular to this plane [9-10].

X-rays can be a useful probe for nozzle cavitation since they can overcome some of the challenges encountered when using visible light. X-rays can penetrate through optically opaque materials, even several millimeters of steel, and still image small bubbles suspended in a fluid [11]. The use of metal nozzles significantly increases the ability to measure cavitation at fluid pressures representative of production fuel injectors. X-rays also have a much smaller probability of scattering at phase boundaries in comparison to visible light, allowing quantification of densities in multiphase flows without the obscuring effect of multiple scattering [12]. For these reasons, several recent studies have used X-rays to study cavitation, including quantifying the density distribution in a cavitating flow [13], imaging cavitation in a steel nozzle [14], imaging cavitation and spray formation inside a near-production gasoline injector

[15], and measurements of the 3D liquid volume fraction distribution in a cavitating nozzle using X-ray tomography [16]. In the current work, several X-ray diagnostics are combined to characterize the internal flow and the external spray formation of a cavitating diesel nozzle under conditions relevant to modern engines. The combination of techniques forms an unprecedented data set for the study of nozzle flows, cavitation, and primary breakup of fuel injection sprays.

Material and methods

The injector of interest in this work is the "Spray C #037" injector from the Engine Combustion Network (ECN). This injector is from a medium-duty diesel engine, but while the production injector has multiple holes, the research-grade Spray C injector has a single hole oriented along the injector's axis. The injector is designed to promote cavitation; very little hydro-erosion was used in its manufacture so that the corners from the nozzle sac to the hole remain relatively sharp. The hole itself has a diameter of approximately 210 μm, and is nearly cylindrical along its length, without the convergence that is typically used to suppress cavitation in modern production injectors. All measurements used the same injector and fuel; n-dodecane at 24°C, spraying into a chamber filled with nitrogen gas at 23°C.

The results of several different experimental diagnostics are presented in this work. Note that these diagnostics cannot resolve between fuel vapor formed as a result of cavitation, and gas ingested from outside the nozzle as a result of hydraulic flip. As will be shown later, in some regions gas appears to be present along the entire length of the nozzle from inlet corner to exit, and this may result in hydraulic flip. Under hydraulic flip, intense cavitation that extends all the way to the end of the nozzle to meet the ambient gas, which, because of its higher pressure, may then move into the nozzle and stabilize the separated flow. Hydraulic flip occurs as a result of very strongly cavitating flows, and for this reason the authors have chosen to refer to regions where gas has been detected inside the nozzle as regions of "cavitation", even though these regions may contain fuel vapor, ambient gas, or a mix of the two.

1. X-Ray Tomography of Injector Nozzle Internal Geometry

X-ray tomography was used to characterize the geometry of the internal flow passages in the fuel injector of interest. These measurements were performed at the 7-BM beamline of the Advanced Photon Source (APS) at Argonne National Laboratory. This facility has been optimized for non-destructive, high resolution measurements of small metal objects. The procedure is described in detail in [17]. In brief, the steel nozzles are mounted on a high precision rotational stage, with the center of rotation aligned with the injector axis. As the nozzle is rotated, X-ray projection images are acquired, for a total of 2,400 images over 180 degrees. The images show bright regions where the X-rays pass through less steel, and darker regions where they pass through more. Computed tomography is applied to these images to reconstruct slices of the geometry at 1,000 positions along the nozzle axis. These slices are used to determine the geometric features of the nozzle, including length, diameter, and radii of curvature at several corners. The slices are also used for segmentation, which uses thresholding to identify each pixel in each slice as either steel or air. The "stack" of segmented slices is then used to generate a point cloud of all the surfaces in the nozzle, and finally the point cloud is converted to a 3D volume.

Measurements of the specific Spray C injector used in this work are documented in detail in [18]. The spatial resolution of the measured geometry is 1.8 μm with a field of view of 2.25 × 1.4 mm, capturing the full nozzle profile as well as part of the sac. Relevant features of the geometry will be highlighted in the following sections.

2. X-Ray Imaging of Cavitation Inside Steel Nozzles

X-ray phase contrast imaging was used to visualize the intensity and extent of cavitation inside the Spray C nozzle. A detailed description of the imaging procedures can be found in [19]. In brief, a collimated beam of X-rays passes through the injector and an image of the injector is projected onto a scintillator which converts from X-ray to visible light. The scintillator is then imaged with a microscope and high-speed camera. The contrast in the images is generated through the sum of two mechanisms. First, some of the X-rays are absorbed, primarily in the steel because of its higher electron density, but also in fuel and air to a much lesser extent; this is absorption contrast. Second, the X-rays refract at density gradients within the sample, giving rise to so-called phase contrast. By Snell's law, refraction is at a minimum when these density gradients are oriented along the path of the X-ray beam, and maximized when the gradients are nearly perpendicular to the X-ray propagation. Because the indices of refraction for X-rays interacting with all materials are very nearly unity, the refraction angles are very small, and only those X-rays which encounter density gradients nearly perpendicular to their direction of travel have their trajectory significantly changed from that of the incident beam. In the image projected onto the scintillator, then, the phase contrast is visible as a very narrow fringe pattern surrounding the density gradients that are perpendicular to the beam.

The images inside the Spray C injector that are presented in this work were conducted at the 32-ID beamline at APS. A high-speed camera fitted with a 5X microscope objective collected 50,000 frames-per-second, gathering

250 frames per injection event, then repeated for 30-40 events to observe shot-to-shot variability and improve signal-to-noise ratio.

3. X-Ray Measurements of Spray Density

Measurements of the density distribution of the fuel jet emerging from the Spray C nozzle were conducted at the 7-BM beamline at APS. A detailed description of the measurement procedures is given in [20]. In brief, the fuel injector was mounted vertically, spraying down into a steel pressure chamber that allows for the full rotation of the injector with respect to the X-ray beam. A monochromator was used to select an X-ray beam energy of 8 keV, this beam was then focused to a beam size of 5 × 6 µm and passed through the spray. As the X-rays pass through the spray, some are absorbed by the fuel according to the Lambert-Beer law, allowing the mass of fuel in the path of the beam to be related to the changing X-ray intensity. The X-ray intensity was measured as a function of time by a PIN diode and recorded at a rate of 271 kHz. The focused beam was raster scanned across the spray at several positions downstream and perpendicular to the injector tip, and at each location the X-ray intensity and thus the projected mass was recorded for 32 individual injection events. After completion of each raster scan, the injector was rotated by 3 degrees, and the process was repeated over 60 rotation angles from 0 to 180 degrees.
Density measurements from the recorded 60 lines of sight were reconstructed into 2D slices using computed tomography. The result of the reconstructions are three time-resolved, ensemble-averaged density fields at distances of 0.1, 2.0, and 5.0 mm downstream of the injector.

4. X-Ray Tomography of Nozzle Cavitation

X-ray phase contrast imaging was combined with computed tomography to obtain 3D distributions of cavitation intensity and extent inside the Spray C nozzle. The injector was mounted in a pressurized spray chamber, with the ability to rotate the injector through 180 degrees. Images of the cavitating flow were acquired with a pixel resolution of 2 µm. The injector was energized to produce an injection duration of 3 ms, and the camera was timed to expose for 1 ms during the steady, middle part of the injection. Images were acquired for 214 injection events at each rotation angle, and the injector was rotated through 180 degrees in 0.5 degree steps. The images from the recorded 360 lines of sight were reconstructed into 2D slices using computed tomography. Each pixel of the slices was then binarized, categorizing each pixel as either gas or as a fluid with higher density. As the phase contrast images have limited ability to quantify density, only the pixels with the highest brightness were categorized as gas, and no attempt has been made to further quantify the density in regions of lower brightness. The categorized slices at each position along the length of the nozzle then show the regions where the presence of gas is steady and reproducible. The measurements are not able to resolve between vapor generated by cavitation and gas from outside the nozzle, which may be present in the nozzle as a result of hydraulic flip.

Results and discussion

Figure 1 shows a cutaway view of the tip of the Spray C injector, which resulted from synchrotron X-ray tomography measurements. This cutaway reveals the outer surface of the injector tip, as well as the tip of the pintle, shape of the sac, entrance to the nozzle, and inner surface of the nozzle itself. Validation of the accuracy and precision of these measurements is documented in [17].

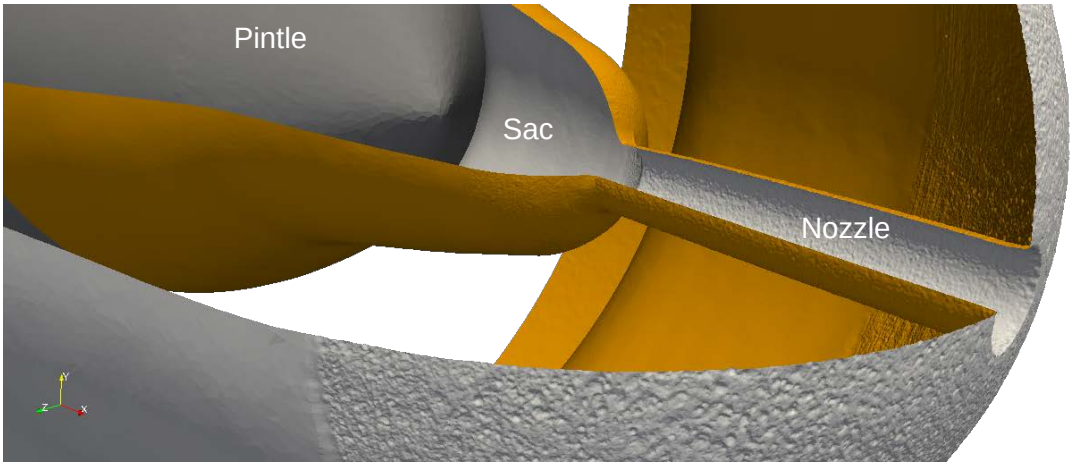

Figure 1. Cutaway view of the tip of the Spray C injector, measured using X-ray tomography.

The high spatial resolution of the geometry measurements allows geometric features of the internal flow passages to be determined with high precision. Figure 2 shows the coordinate system used in this work (left), the measured hole radius as a function of position (center), and the measured radius of curvature of the inlet corner (leading from the sac to the nozzle) as a function of azimuthal angle (right). The measured radii for Spray C reveal a hole whose

radius increases slightly in the direction of flow. The measurements of inlet corner radius show a relatively sharp inlet corner when this injector is compared to its Spray D analog [18], as well as significant variation of the radius of curvature depending on the azimuthal location. The minimum radius of curvature (sharpest inlet corner) is near the 0°/360° location while the maximum is near 180°. Local minima and maxima in the radius of curvature are also observed, these indicate the presence of “grooves” in the geometry that cause a local increase in the corner radius at approximately ten azimuthal locations. Geometric features such as those described here are known to influence the flowfield and encourage or suppress cavitation [21,22].

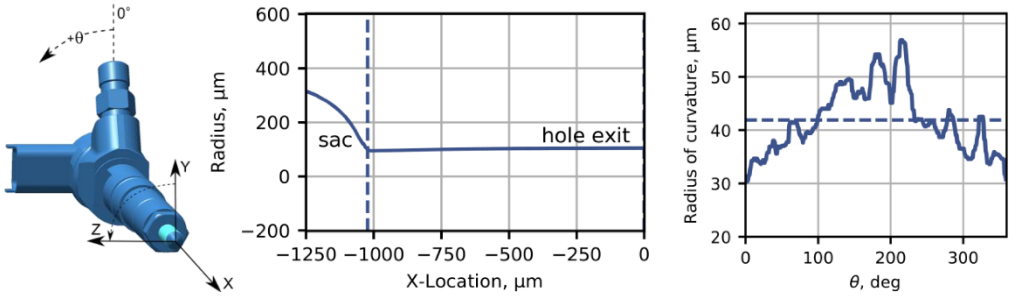

Figure 2. The coordinate system used in this work (left) [23], the average measured hole radius as a function of position (center), and the radius of curvature of the inlet corner as a function of azimuthal angle (right).

Figure 3 shows time-averaged X-ray phase contrast images through the Spray C injector, collected at an injection pressure of 150 MPa with an ambient environment outside the injector of 2 MPa N_2 gas. The images were acquired during the steady portion of each injection sequence. They were post-processed to highlight the differences between fuel and gas inside the nozzle during an injection event. The processing method highlights all signal variation between the no-flow period and the steady injection phase; this includes motions of the injector which manifest themselves as intensity variations at the edges of the sac and hole.

Gas inside the nozzle as a result of cavitation can be clearly seen in Figure 3(a) inside the upper portion of the nozzle, which corresponds to the θ = 0° azimuthal position of the injector. As shown in Figure 2, this region with maximum cavitation corresponds to the inlet corner with the smallest radius of curvature. In contrast, the θ = 180° entrance corner shown in the lower part of Figure 3(a) corresponds to the largest inlet corner radius (Figure 2) and shows no evidence of cavitation.

The gas visible at the θ = 0° location grows rapidly from the entrance corner to a thickness of 47 µm at 200 µm downstream and 74 mm by 600 mm downstream, covering ~38% of the hole diameter.

In Figure 3(b), the injector has been rotated by 90° from the view in 3(a). This orthogonal view shows the cavitation arising from the inlet corners at θ = 90° (upper) and θ = 270°. These corners, with radius of curvature near the average of 42 µm, show significantly less cavitation than the θ = 0° corner, and more than the θ = 270° corner, with cavitation reaching a maximum thickness in this view of 27 µm and thinning as the flow moves downstream.

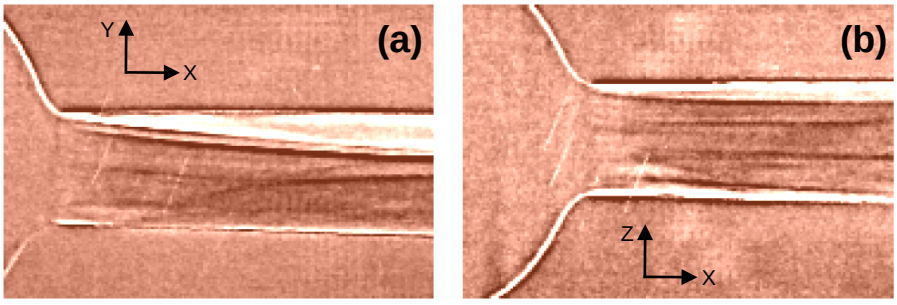

Figure 3. Phase contrast images of the steady-state nozzle flow from two different lines-of-sight through the Spray C injector.

Figure 4 shows the steady-state projected density profiles of the fuel jet emerging from the Spray C nozzle at distances of 0.1, 2, and 5.0 mm downstream of the nozzle exit, measured at an injection pressure of 150 MPa in an ambient environment of 2 MPa N_2 gas. Figure 4(a) clearly shows the asymmetric nature of the fuel distribution caused by the presence of cavitation inside the Spray C nozzle. The region of gas inside the nozzle observed in Figure 3(a) occludes a portion of the hole exit, creating a fuel distribution that is significantly different than the shape of the nearly-circular steel nozzle.

Note that the maximum density measured in the fuel jet at 0.1 mm downstream of the nozzle is ~690 μg/mm^3. This maximum is present in a localized region of the fuel distribution, visible as a yellow spot in the lower left of the orange field. The average fuel density across the field is ~600 μg/mm^3. This is significantly below the density of pure liquid dodecane, 750 μg/mm^3 at 20°C [24]. There are several possible explanations. First, the process of ensemble averaging that is inherent in this data may cause any dynamic changes in the fuel distribution, such as spray motion or localized pockets of gas or vapor, to be averaged across the distribution, decreasing the observed density. Second, the fuel temperature may have increased during its path through the nozzle, lowering the density. The authors expect this second explanation to be unlikely, as a temperature increase of ~175°C would be required to decrease the density to the measured value [25].

The downstream measurements reflect the influence of the initially-skewed distribution upstream; a low-density region persists in the upper part of Figure 4(b) due to in-nozzle cavitation and the resulting restriction in fuel flow. As the spray moves farther downstream, Figure 4(c) shows that by 5 mm, the spray is broadly dispersed vertically; cavitation is promoting rapid mixing and jet growth, but it occurs preferentially along the spray periphery and it is particularly aligned with the sharp inlet corner of the nozzle.

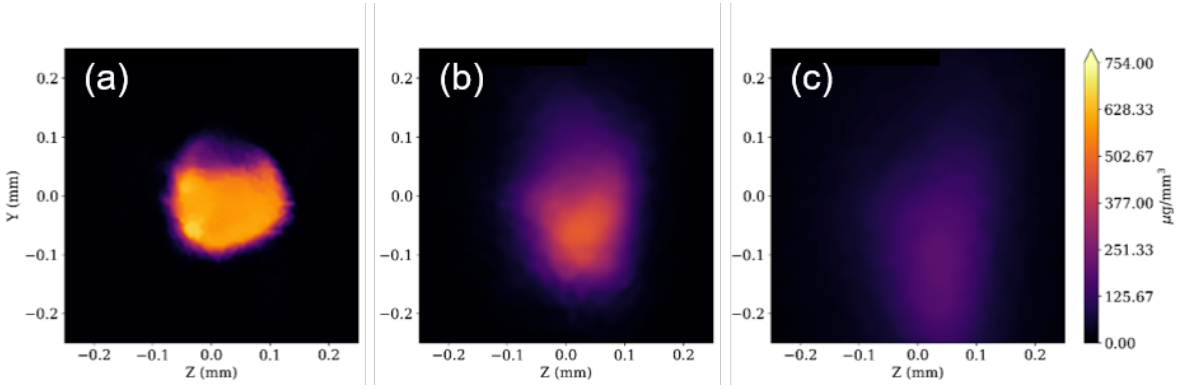

Figure 4. Steady-state projected density profiles of the fuel jet emerging from Spray C at 0.1 (a), 2.0 (b), and 5.0 (c) mm downstream of the nozzle.

Figure 5 shows six cross sections through the cavitating flow in the Spray C nozzle. These were measured using tomographic reconstructions of X-ray phase contrast images from many lines of sight through the nozzle, with the images time-gated on the steady part of the spray. While only six cross sections are shown, similar distributions were measured at 990 locations in the nozzle, spanning from the inlet corner to the nozzle exit.

The distributions show that the regions of gas are located along the nozzle wall as expected. In the upstream portions of the nozzle, gas is found along the nozzle wall from approximately θ = -90° to θ = 90°, with the thickest extent near θ = 0°, consistent with the planar cavitation images shown in Figure 3. As the flow continues downstream, the azimuthal extent of cavitation with a thickness more than a few microns becomes narrower, but remains strong at θ = 0° all the way to the nozzle exit.

One interesting feature in Figure 5 is that there appears to be at least a thin layer of cavitation at all azimuthal values all the way to the nozzle exit. The current work cannot confirm that these thin regions near the wall are truly a result of cavitation or separated flow, since small nozzle motions could cause the same effect. However, cavitation in this region of the nozzle would not be unexpected in a nozzle geometry that is diverging along its entire length, as has been found in this Spray C nozzle.

The spatial resolution of these reconstructions is approximately 5 μm. The lower limit for detecting cavitation using this tomographic method is still unknown; the authors are considering methods to quantify this in the future.

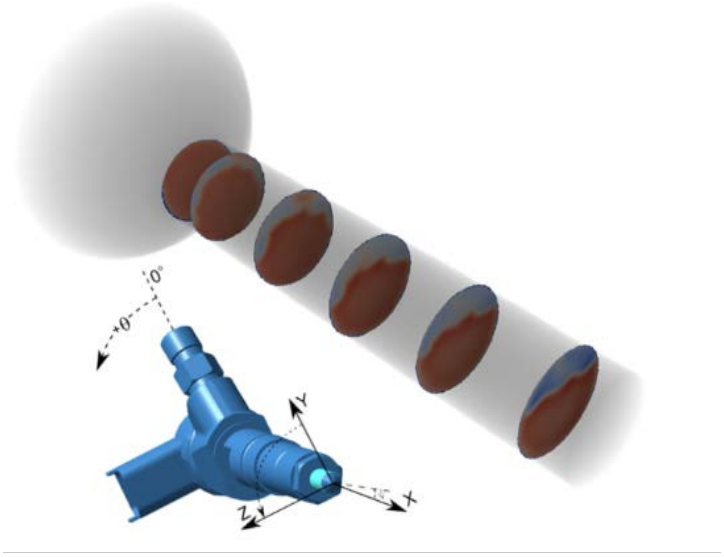

Figure 5. Cross sections showing the steady-state cavitation distribution in the Spray C nozzle.

Conclusions

This work investigated the influence of asymmetric injector nozzle geometry on the occurrence of cavitation and its ultimate effect on spray behavior. X-ray diagnostics were used to investigate the internal and near-nozzle flow in the ECN Spray C injector. The internal geometry was measured with 1.8 µm spatial resolution, revealing a sharp, asymmetric nozzle inlet corner. Both 2D and 3D imaging techniques were used to determine the distribution of cavitation inside the nozzle. The location of the smallest inlet corner radius of curvature corresponded directly to the location of the most intense and extensive cavitation during the steady part of the spray. Little or no cavitation was observed in parts of the nozzle with a larger inlet radius of curvature. The presence of cavitation strongly influenced the resulting fuel spray structure, with significant deficit of fuel in the near-nozzle regions of the fuel jet that align with the strongest internal cavitation. Fuel distributions farther downstream indicate a widening of the fuel spray that is also oriented toward the regions of strongest cavitation.

These observations illustrate the influence cavitation has on spray breakup, which in turn can affect combustion and engine performance. Together, this comprehensive data set quantifies the nozzle geometry, tracks its effect on internal nozzle cavitation, and the ultimate influence on the external fuel distribution, all in a geometry that is representative of production nozzles at realistic pressure conditions. The data sets are freely available [26] and should prove valuable for the development and validation of computational models simulating nozzle flow, cavitation, and primary atomization of sprays.

Acknowledgements

Research presented in this paper was performed at the 7-BM and 32-ID beamlines at the Advanced Photon Source at Argonne National Laboratory. Use of the APS is supported by the U.S. Department of Energy (DOE) under Contract No. DEAC0206CH11357. Argonne's research on fuel injection, sprays, and combustion is sponsored by the DOE Vehicle Technologies Program under the direction of Gurpreet Singh and Michael Weismiller.

Nomenclature

ECN	Engine Combustion Network
APS	Advanced Photon Source

References

[1] Bergwerk, W., 1959, Proceedings of the Institution of Mechanical Engineers, 173 (1), pp. 655–660.
[2] Lopez, J. J., de la Garza, O. A., De la Morena, J. Martínez-Martínez, S., 2017, International Journal of Engine Research, 18 (10), pp. 1017–1034.
[3] Payri, R., Gimeno, J., Cuisano, J., Arco, J., 2016, Fuel 180, pp. 357-366.
[4] Westlye, F. R., Battistoni, M., Skeen, S. A., Manin, J., Pickett, L. M., Ivarsson, A., 2016, SAE Technical Paper 2016-01-0860.
[5] Duke, D. J., Kastengren, A. L., Matusik, K. E., Powell, C. F., 2019, International Journal of Multiphase Flow, In Press.
[6] Bush, D., Soteriou, C., Winterbourn, M., Daveau, C., 2015, Journal of Physics: Conference Series. 656 012080.

[7] Gavaises, M., Villa, F., Koukouvinis, P., Marengo, M., Franc, J.P., 2014, International Journal of Multiphase Flow 68, pp. 14-26.
[8] Chaves, H., Miranda, R., Knake, R., Jul. 9-13 2007, 6th International Conference on Multiphase Flow.
[9] Sou, A., Hosokawa, S., Tomiyama, A., 2010, Atomization and Sprays 20 (6), pp. 513–524.
[10] He, Z., Chen, Y., Leng, X., Wang, Q., Guo, G., 2016, International Communications in Heat and Mass Transfer 76 pp. 108-11.
[11] Swantek, A. B., Kastengren, A. L., Duke, D. J., Tilocco, F. Z., Sovis, N., Powell, C. F., Sep. 8-10 2014, 26th European Conference on Liquid Atomization and Spray Systems.
[12] Kastengren, A. L., Powell, C. F., 2014, Experiments in Fluids 55 (1686).
[13] Daniel J Duke, D. J., Matusik, K. E., Kastengren, A. L., Swantek, A. B., Sovis, N., Payri, R., Viera, J. P., Powell, C. F., 2017, International Journal of Engine Research, 18 (1–2), pp. 39–50.
[14] Moon, S., Komada, K., Li, Z., Wang, J., Kimijima, T., Arima, T., Maeda, Y., Aug. 23-25 2015, 13th Triennial International Conference on Liquid Atomization and Spray Systems.
[15] Sou, A., Minami, S., Prasetya, R., Pratama, R., Moon, S., Wada, Y., and Yokohata, H., Aug. 23-25 2015, 13th Triennial International Conference on Liquid Atomization and Spray Systems.
[16] Mitroglou, N., Lorenzi, M., Santini, M., Gavaises, M., 2016, Experiments in Fluids 57 (175).
[17] Matusik, K. E., Duke, D., J., Kastengren, A. L., Sovis, N., Swantek, A. B., Powell, C. F., 2017, International Journal of Engine Research, 19 (9), pp. 963–976.
[18] Sforzo, B. A., Matusik, K. E., Powell, C. F., Kastengren, A. L., Daly, S., Skeen, S., Cenker, E., Pickett, L. M., Crua, C., and Manin, J., May 14-16 2018, The 10th International Symposium on Cavitation.
[19] Duke, D., Swantek, A., Tilocco, Z., Kastengren, A., Fezzaa, K., Neroorkar, K., Moulai, M., Powell, C. F., and Schmidt, D., 2014, SAE International Journal of Engines 7 (2) pp. 1003–1016.
[20] Matusik, K. E., Duke, D. J. Sovis, N., Swantek, A. B., Powell, C. F., Payri, R., Vaquerizo, D., Giraldo-Valderrama, S. Kastengren, A. L., Sep. 6-8 2017, 28th European Conference on Liquid Atomization and Spray Systems.
[21] Chaves, H. and Ludwig, C., Sep. 4-7 2005, 20th European Conference on Liquid Atomization and Spray Systems.
[22] Schmidt, D. P., Rutland, C., Corradini, M., Roosen, P., and Genge, O., 1999, SAE Technical Paper 1999-01-0518.
[23] Sandia National Laboratories, Engine Combustion Network. https://ecn.sandia.gov
[24] CRC Handbook of Chemistry and Physics, 66th Edition, Robert C. Weast, Editor, page C-254.
[25] Trusler, M., Wakeham, W. A., 2004, International Journal of Thermophysics 25 (5), pp.1339-1352.
[26] X-Ray Spray Research Data Sharing, Argonne National Laboratory, https://anl.box.com/v/XRaySpray ([cit. 2019-03-31]).